Modeling Terrestrial Biogenic Sources of Oxygenated Organic Emissions

Christopher Potter

NASA Ames Research Center, Moffett Field, California

Steven Klooster

California State University, Monterey Bay, Seaside, California

David Bubenheim and Hanwant B. Singh

NASA Ames Research Center, Moffett Field, California

Ranga Myneni

Boston University, Boston, Massachusetts

Received 11 February 2003; accepted 17 April 2003

ABSTRACT: In recent years, oxygenated volatile organic chemicals (OVOCs) like acetone have been recognized as important atmospheric constituents due to their ability to sequester reactive nitrogen in the form peroxyacetyl nitrate (PAN) and to be a source of hydroxyl radicals (HO_x) in critical regions of the atmosphere. The potential biogenic sources of acetone include terrestrial plant canopies, oxidation of dead plant material, harvest of cultivated plants, biomass burning, and the oceans. These sources are poorly con-

* Corresponding author address: C. Potter, NASA Ames Research Center, Moffett Field, CA
E-mail address: cpotter@mail.arc.nasa.gov

strained at present in budgets of atmospheric chemistry. Based on reported laboratory, field, and satellite observations to date, an approach is presented for a biosphere model to estimate monthly emissions of acetone from the terrestrial surface to the atmosphere. The approach is driven by observed land surface climate and estimates of vegetation leaf area index (LAI), which are generated at 0.5° spatial resolution from the NOAA satellite Advanced Very High Resolution Radiometer (AVHRR). Seasonal changes in LAI are estimated using the Moderate Resolution Imaging Spectroradiometer (MODIS) radiative transfer algorithms to identify the probable times and locations of crop harvest in cultivated areas and leaf fall of newly dead plant material in noncultivated areas. Temperature-dependent emission factors are applied to derive global budgets of acetone fluxes from terrestrial plant canopies, oxidation of dead plant material, and harvest of cropland plants. The predicted global distribution of acetone emissions from live foliage is strongly weighted toward the moist tropical zones, where relatively warm temperatures and high LAI are observed in rain forest areas year-round. Predicted acetone emissions are estimated at between 54 and 172 Tg yr^{-1} from live foliage sources and between 7 and 22 Tg yr^{-1} from decay of dead foliage. These flux totals from vegetation are large enough to account for the majority of postulated biogenic acetone sources in models of global atmospheric chemistry, but our model predictions are subject to verification in subsequent flux control experiments using a variety of plant species, particularly those from humid tropical zones.

KEYWORDS: Acetone, Biosphere, Model

1. Introduction

Oxygenated volatile organic chemicals (OVOCs) have been found to be ubiquitous and abundant components of the global troposphere (Singh et al., 2001). Among the myriad of such chemicals present, acetone and methanol are the most dominant. Acetone has been recognized as an important compound in atmospheric chemistry because it can sequester reactive nitrogen in the form of peroxyacetyl nitrate (PAN, $CH_3CO_2ONO_2$) and provide a direct source of hydroxyl radicals HO_x ($OH+HO_2$) in the upper troposphere (Singh et al., 1995). These acetone-initiated reactions can substantially alter the rates of ozone formation in the upper troposphere (Wennberg et al., 1998; Collins et al., 1999; Muller and Brasseur, 1999), and therefore play a role in the Earth's radiation balance. The sources and sinks of OVOCs are poorly known but biogenic emissions are thought to provide an important source.

Recent assessments have projected that between 300 and 500 Tg of OVOCs are emitted into the atmosphere every year (Guenther et al., 1995; Fall, 1999). Large fractions of emissions are suspected to be biogenic in origin, including about 30–40 Tg yr^{-1} of acetone directly from terrestrial biogenic sources, excluding biomass burning and oxidation of organic precursors (Singh et al., 2000; Singh et al. 2001; Jacob et al., 2002). Development of accurate, seasonally resolved emission inventories, ideally based on high-resolution ecological mapping studies, is crucial to the improvement of global atmospheric model simulations and the consistency between these model predictions and atmospheric measure-

ments of acetone concentrations. However, no global gridded acetone or methanol emissions inventories have yet been provided through cooperative international research programs, such as the Global Emissions Inventory Activity (GEIA) component of the International Global Atmospheric Chemistry (IGAC) Project, a core project of the International Geosphere–Biosphere Program, or through the Emission Database for Global Atmospheric Research (EDGAR; Olivier et al., 2001).

There have been only a few published measurements for biogenic emissions of acetone and methanol. Previously reported rates of acetone emission (from apparently undamaged plant tissues) range from 0.01 to 0.5 μg g^{-1} h^{-1}, whereas emission rates for methanol can exceed 10 μg g^{-1} h^{-1} (MacDonald and Fall, 1993). Land cover and land-use change may be particularly important factors to include for accurate estimation of OVOC emissions on regional scales. Cutting and dehydration of plant material in crop and timber harvest areas, lawn mowing, and range land grazing are some of the major human activities that are thought to impact global OVOC emissions (Fall, 1999; de Gouw et al., 1999).

The aim of this study is to develop an approach for the first fully integrated global model to predict monthly biosphere–atmosphere fluxes of OVOC, with particular emphasis on major terrestrial vegetation sources of acetone.

Our specific objectives are to address the following research questions.

1. How do regional OVOC emissions vary with temperature, moisture availability, and vegetation properties?
2. How do regional OVOC emissions vary with plant tissue damage or plant harvest by cutting?
3. How can predicted OVOC emissions be scaled up to regional and global levels using remote sensing (satellite) data to drive ecosystem carbon models?

2. Modeling approach

2.1. Acetone emission algorithms

Here we describe the concept and algorithm development for a generalized model of biogenic OVOC emissions directly from terrestrial ecosystems. The model considers emissions from intact (living) plant canopies, decaying plant material, and harvested plant material from agricultural ecosystems. We have not considered emissions from the oxidation of organic precursors.

For the most part, OVOC emission measurements in plant and ecosystem field studies to date suggest that emission rates are controlled primarily by temperature effects on leaf growth and respiration metabolism (Fall, 1999). Relative humidity and radiation flux could be secondary controllers of these emissions, but their importance is poorly understood at present. Consequently, the OVOC emission algorithms we describe here are developed primarily as functions of basal emission rates (measured at 303 K), adjusted by the density of foliar biomass, a vegetation-specific emission coefficient, and an exponential temperature response. Based chiefly on measurements reported by Schade and Goldstein (Schade and Goldstein, 2001) and deGouw et al. (deGouw et al., 1999), we define terrestrial OVOC source emissions by the following generalized algorithms.

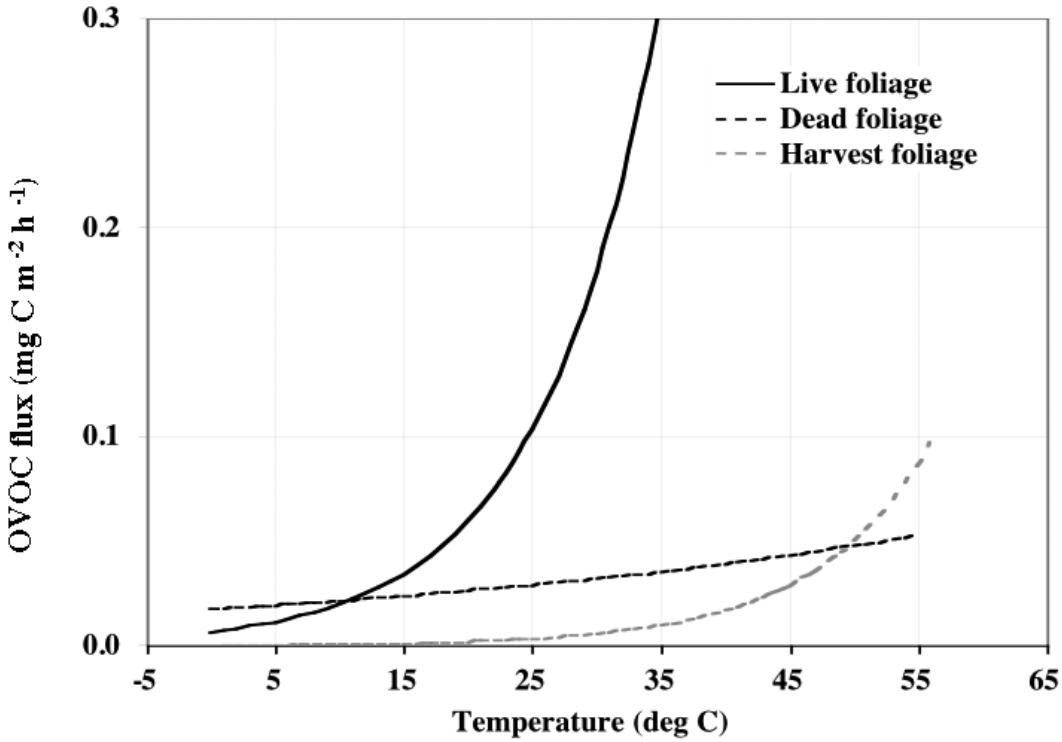

Figure 1. Comparison of OVOC emission equations for acetone as functions of temperature, based on parameter definitions from Schade and Goldstein (Schade and Goldstein, 2001)

Intact plant canopies (live foliage),

$$F_{\mathrm{lf}} = \varepsilon\, D_{\mathrm{lf}} \exp[\beta\,(T_a - T_{\mathrm{ref}})]. \quad (1)$$

Decaying plant material (dead foliage),

$$F_{\mathrm{df}} = \varepsilon\, D_{\mathrm{df}} \exp[\beta\,(T_a - T_{\mathrm{ref}})]\, P. \quad (2)$$

Harvested plant material (harvest foliage),

$$F_{\mathrm{ht}} = \varepsilon\, D_{\mathrm{ht}} \exp[\beta\,(T_a - T_{\mathrm{ref}})]. \quad (3)$$

Here F emission fluxes (in mg m^{-2} h^{-1}) are adjusted to monthly flux totals; ε is the OVOC-specific base emission rate (in mg m^{-2} h^{-1} at 303 K); D is the scaling factor for live foliar density, dead organic matter density, or harvested foliar density [in units of leaf area index (LAI), m^2 m^{-2}]; β is the vegetation-specific emission coefficient; T_a is surface air temperature (K); $T_{\mathrm{ref}} = 303$ K; and P is the coefficient for rainfall wetting effects on emissions from decaying plant material ($P=1$, if rainfall < 1 cm in a month; $P=2$, if rainfall ≥ 1 cm in a month).

A comparison of the three OVOC emission equations as functions of temperature is shown in Figure 1. For acetone and methanol emissions, Schade and

Goldstein (Schade and Goldstein, 2001) reported β values for live foliage that were several times larger than β values for dead foliage (Table 1). This results in a more rapid exponential increase in emission rates with increasing temperature in the live foliage response function than in the dead foliage response function. Lacking more specific information, Equation (3) for harvest foliage emission uses the same β values as Equation (1) for live foliage.

Table 1. Parameter values for OVOC emissions, as defined in Equations (1)–(3). All reported values of ε base emission rates have been normalized to LAI=1, and are reported in units of mg C m^{-2} h^{-1} at 303 K. The vegetation-specific emission coefficient is denoted by β. *Pinus ponderosa* values are from Schade and Goldstein (Schade and Goldstein, 2001). *Trifolium ripens* values are from Gouw et al. (Gouw et al., 1999). Mixed herbs values are from Fukui and Doskey (Fukui and Doskey, 1998). NA is not available.

		Live foliage		Dead foliage		Harvested foliage	
Species	OVOC	ε	β	ε	β	ε	β
Pinus ponderosa	Acetone	0.176	0.110	0.032	0.020		
Pinus ponderosa	Methanol	1.367	0.110	0.032	0.030		
Pinus ponderosa	Ethanol	0.305	0.140	NA	NA		
Trifolium ripens	Acetone					0.00608	NA
Trifolium ripens	Methanol					0.00152	NA
Mixed herbs	Acetone	0.047					
Mixed herbs	Methanol	0.157					

In all cases, we have normalized the reported base emission rate values of ε to LAI=1. The D scaling factor can then be applied to multiply emissions up to full vegetation canopy levels. For example, LAI for *ponderosa pine* has been reported by Schade and Goldstein (Schade and Goldstein, 2001), which has been used as a scaling factor for other grid cells (using remotely sensed LAI).

The algorithm for OVOC emissions from decaying plant material [Equation (2)] is based on the assumption that emission from dead foliage derives mainly from organic material that has fallen onto the soil surface within the past year. These emissions would involve relatively rapid microbial decomposition of the most labile foliar compounds, leaving behind mainly structural leaf components such as cellulose and lignin that can remain in the soil organic horizons for years afterward in a relatively inert state. If this assumption is correct, then we can estimate the density and monthly timing of dead foliage transferred from live vegetation to the soil surface within the past year as a function of the maximum LAI value measured over the course of the year, multiplied by the monthly percent of annual leaf fall total. To compute the monthly D scaling factor in Equation (2), we use the formulation from Potter et al. (Potter et al., 1993) to compute the monthly percent of leaf fall based on a normalized seasonal profile of LAI values. Because this formulation for predicting the monthly percent of leaf fall is based on satellite remote sensing of global vegetation dynamics (see section 2.2), we have the potential to capture many effects of large-scale natural disturbance events such as major wind storms, and frost, hail, and ice damage on the transfer of live to dead foliage pools.

Although corroborating evidence on moisture effects is not well developed,

Warneke et al. (Warneke et al., 1999) reported that acetone emission rates from dead plant material were doubled when rainfall was recorded in a preceding 24-h period. We have included this presumed effect of wetting on rates of microbial decay of dead plant material and OVOC emissions using the monthly precipitation amount as an index of moisture delivered to the layers of dead plant material decaying on the soil surface. Studies of rainfall interception in mature forests generally indicate that vegetation canopies have a maximum storage capacity of about 0.2 cm of rainfall (Federer, 1979). For soil surface layers to remain moist throughout a monthly time interval, multiple rainfall events greater than 0.2 cm are necessary to offset evaporative losses. Therefore, a threshold value of rainfall ≥ 1 cm month^{-1} was set in Equation (2) as a general index for wet season (versus dry season) moisture effects on decay rates of dead plant material on the soil surface.

Emissions from harvested foliage are treated separately from naturally decaying foliage because laboratory measurements suggest that intentional damage to previously intact live foliage can result in a transient but significant increase in OVOC emission rates (Kirstine et al., 1998). This potential crop harvest source for acetone therefore results from anthropogenic activities that lead to the wounding of cultivated plant foliage at the end of a crop growing season. On the basis of measurements reported by deGouw et al. (deGouw et al., 1999), it is assumed that harvest emissions have a maximum duration of 7.5 h. This maximum duration time of elevated emissions following crop harvest is close to or slightly longer than duration times for elevated emissions of a variety of VOC compounds reported in other leaf wounding experiments (Fall et al., 1999). We note that the harvest foliage source [Equation (3)] for OVOC does not include the subsequent decay source from crop residues in the months following harvest.

2.2. Satellite and climate input datasets

Global climate drivers for our OVOC emission model include monthly mean surface temperature and precipitation amount. These model inputs are long-term (1931–60) averages gridded at 0.5° spatial resolution (Legates and Willmott, 1990). The climatology was developed using a database of 17,986 independent terrestrial station records and 6955 oceanic gridpoint records. Weather station data were interpolated to a 0.5° latitude–longitude grid using a spherically based interpolation algorithm.

Global vegetation cover types in the model were determined by DeFries et al. (DeFries et al., 1998) on the basis of differences in seasonal profiles of the Normalized Difference Vegetation Index (NDVI) gridded at 0.5° resolution. NDVI is a unitless parameter (scaled from 0 to 1000) computed from the ratio of visible (VIS) and near-infrared (NIR) sensor channels. Global coverage of NDVI is obtained from the Advanced Very High Resolution Radiometer (AVHRR) satellite sensor as this VIS:NIR channel ratio. As a terrestrial ‘‘greenness’’ index, the AVHRR NDVI has been closely correlated with a variety of vegetation parameters, including canopy LAI (Running and Nemani, 1988; Sellers et al., 1994; DeFries et al., 1995).

For derivation of LAI at 0.5° spatial resolution, nearly complete AVHRR

datasets for the 1980s and 1990s have been produced from the National Atmospheric and Oceanic Administration (NOAA) Global Area Coverage (GAC) Level 1B data. These data consist of reflectances and brightness temperatures derived from the five-channel cross-track scanning AVHRR aboard the NOAA Polar Orbiter ''afternoon'' satellites (*NOAA-7, -9, -11,* and *-14*). Monthly composite datasets remove much of the contamination due to cloud cover present in the daily AVHRR data (Holben, 1986). Nevertheless, additional processing of the satellite imagery is necessary to eliminate remaining artifacts (Los et al., 1994). These data show minimal correlations with equatorial crossing times of the NOAA satellites (Malmström et al., 1997), which suggests that corrections have been made for orbital drifts and switches between satellites (e.g., *NOAA-9* to *NOAA-11*).

The input of live foliar density values to our model [Equation (1)] is made in terms of LAI derived from modified Moderate Resolution Imaging Spectroradiometer (MODIS) radiative transfer algorithms (Buermann et al., 2001), using the Global Invenory Monitoring and Modelling System (GIMMS) AVHRR data from 1982 to 1999. The global MODIS algorithm products we use include improved calibration for intra- and intersensor variations, partial atmospheric correction for gaseous absorption and scattering, and correction for stratospheric aerosol effects associated with volcanic eruptions. The three-dimensional transport equation based on an atmospherically corrected bidirectional reflectance distribution function (BRDF) is used to simulate canopy reflectances using sun-angle geometry and canopy/soil patterns as fundamental inputs. These advances are significant because (i) NDVI relations are sensitive to changes in sun angle, view angle, and background reflectance, while the MODIS algorithm actually exploits these changes to retrieve LAI; and (ii) the NDVI-based algorithm can only use two spectral bands, while the MODIS algorithm can ingest all the available spectral information to improve the quality of retrievals (Knyazikhin et al., 1998).

The monthly fraction of canopy litterfall and amounts of dead foliage transferred to the soil surface for decay [for Equation (2)] were computed using the formulation of Potter et al. (Potter et al., 1993) using seasonal profiles of MODIS algorithm LAI at 0.5° spatial resolution from global average AVHRR data, as reported by Buermann et al. (Buermann et al., 2001). The month of crop harvest at 0.5° spatial resolution was determined from the maximum monthly percent of leaf fall computed from the seasonal LAI-based formulation of Potter et al. (Potter et al., 1993) for those areas of the land surface classified as croplands by DeFries et al. (DeFries et al., 1998). This cropland cover class delineated by DeFries et al. (DeFries et al., 1998) does not include tree harvest areas or expansive range lands that are grazed periodically by livestock. Therefore, we could not yet include the effects of timber cutting, ''slash and burn'' deforestation, nor livestock damage to foliage in the equation [Equation (3)] for harvest-related emissions of OVOC.

3. Global model results

Peak predicted emissions of acetone from live foliage occur during the period of July–August from a variety of forested ecosystems (Figure 2). Temperate deciduous forests exhibit the most pronounced seasonal cycle in predicted acetone

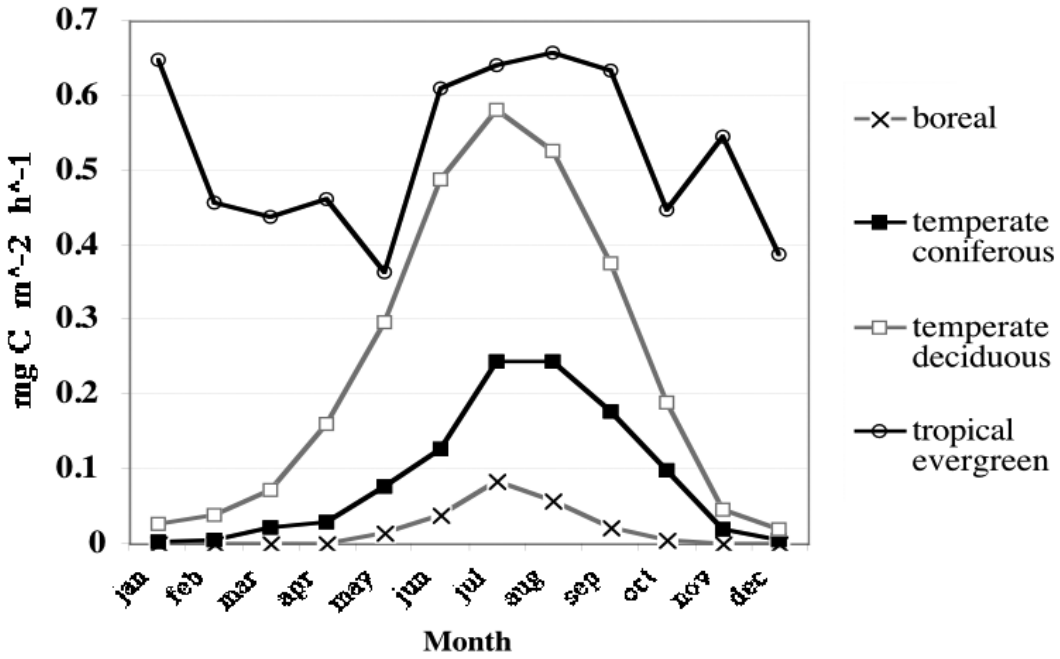

Figure 2. Predicted monthly fluxes of acetone from live foliage at four selected forest sites: boreal coniferous (Manitoba, Canada); temperate coniferous (Thompson, OR, United States); temperate broadleaf deciduous (Coweeta, NC, United States); tropical broadleaf evergreen (Manaus, Brazil).

emissions, owing to the combined effect of warm summers/cold winters and leaf shedding in the fall. Tropical evergreen forests are predicted to respond most notably to seasonal changes in leaf area coverage rather than temperature.

Predicted global emission of acetone from live foliage [Equation (1)] range from 54 to 172 Tg yr^{-1} , depending on the selected setting for ε, the base emission rate (Table 2). Because there are not enough measurement datasets that include ε values to make a separate vegetation-specific assignment for each class in the land cover system of DeFries et al. (DeFries et al., 1998), our annual acetone emission totals are based on the assumption of globally uniform ε values, from the lower estimate of 54 Tg yr^{-1} using uniform ε values for ''mixed herb'' vegetation, to the higher estimate of 172 Tg yr^{-1} using uniform ε values for coniferous forest vegetation (Table 1). In either case of a uniform ε setting, the global distribution of acetone emissions from live foliage is strongly weighted toward the moist tropical zones between 23°N and 23°S latitude (Figure 3a). This zonal pattern derives from relatively warm temperatures and high LAI observed in tropical rain forest areas year-round.

Predicted acetone emissions from dead foliage were estimated at 22 Tg yr^{-1} (Table 2). The global distribution of acetone emissions from dead foliage is close

to being evenly weighted between the areas of northern latitude zones (above 45°N) and moist tropical zones (Figure 3b). Predicted acetone emissions totals from dead foliage are influenced by wide seasonal variations in temperature in the northern latitudes, and by the relative supply and autumn timing of dead leaf material delivered to the soil surface.

Table 2. Predicted acetone emissions from global land cover types. Live foliage emissions are reported for two settings of the base emission rate, ε (Table 1): "Low" from Fukui and Doskey (Fukui and Doskey, 1998) and "High" from Schade and Goldstein (Schade and Goldstein, 2001). Dead foliage emissions are reported for two possible settings of P as defined in Equation (2).

Land cover class (DeFries et al., 1998)	Land area ($km^2 \times 10^6$)	Live foliage: Acetone emission ($Tg\ yr^{-1}$)		Dead foliage: Acetone emission ($Tg\ yr^{-1}$)	
		Low	High	$P = 1$ or 2	$P = 1$
Broadleaf evergreen forest	14	25.8	82.6	6.1	1.9
Coniferous evergreen forest	13	2.7	8.6	3.0	1.0
High-latitude woodland	5.7	0.4	1.3	0.7	0.2
Tundra	7	0.1	0.4	0.3	0.1
Mixed deciduous–evergreen forest	6.6	2.1	6.7	1.9	0.6
Wooded grassland and savanna	22	12.8	40.9	4.6	1.8
Temperate grassland	21	2.2	7.1	1.3	0.5
Bare ground	17	0.1	0.2	0.0	0.0
Cropland	13	3.8	12.0	2.4	0.8
Broadleaf deciduous forest	3	3.3	10.7	1.5	0.5
Shrubs and bare ground	11	0.6	1.8	0.2	0.1
Total	133	54	172	22	7

Owing to uncertainties in reported moisture controls on emissions from dead foliage, we tested the implications of overestimating the available moisture control on OVOC emissions by a setting $P = 2$ for all months when monthly precipitation amount is ≥ 1 cm. Using instead a globally uniform setting of $P=1$ in Equation (2), the predicted acetone source from dead foliage dropped to 7 Tg yr^{-1}. We find that these results are fairly sensitive to the precipitation ≥ 1 cm $month^{-1}$ threshold, because most productive areas of the land receive precipitation in excess of this threshold.

Predicted acetone emissions from cropland harvest sources were relatively small at 16.9×10^6 g yr^{-1}. We find that this predicted OVOC contribution is not large enough on a global basis to significantly augment predicted acetone emissions from dead foliage in noncropland ecosystems, especially in the temperate climate zones. We hypothesize that neither the global extent of cropland harvest areas nor the relatively short duration (several hours) of elevated OVOC emissions following leaf wounding is large enough to make up important contributions to the combined biosphere sources of acetone emissions to the atmosphere. This hypothesis may be proven false if most OVOC emissions from live and dead foliage sources are found not to be active year-round, 24 h day^{-1}.

To demonstrate the versatility of this modeling approach and report an additional prediction for OVOC emissions from live foliage sources, we repeated

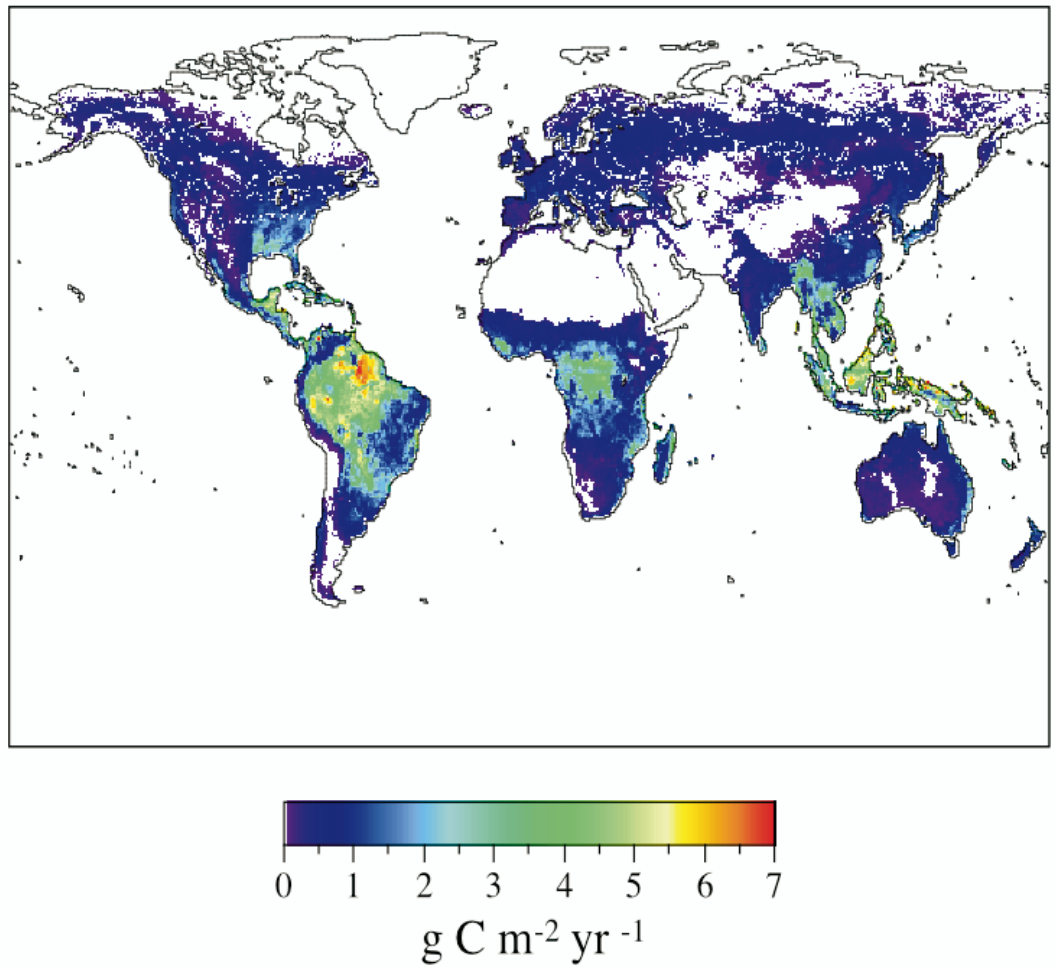

Figure 3. Predicted acetone emissions (in g C m^{-2} yr^{-1}) from (a) live foliage and (b) dead foliage.

the global model computations for methanol emissions with Equation (1), using the ε base emission parameter value reported from Fukui and Doskey (Fukui and Doskey, 1998) and the β emission parameter value reported from Schade and Goldstein (Schade and Goldstein, 2001; Table 1). Global biogenic sources from live foliage for methanol are predicted at 254 Tg yr^{-1} using this model. Our predicted annual emission source from the terrestrial biosphere approaches earlier predictions from Guenther et al. (Guenther et al., 1995), who suggested the primary biogenic source is more than 280 Tg yr^{-1} of methanol. However, Holzinger et al. (Holzinger et al., 2000) have reported a laboratory study with Mediterranean holm oak that shows about one-tenth the methanol emissions reported by others for alfalfa, soybeans, pines/conifers, and aspen, suggesting the need for further measurements of ε and β parameter values.

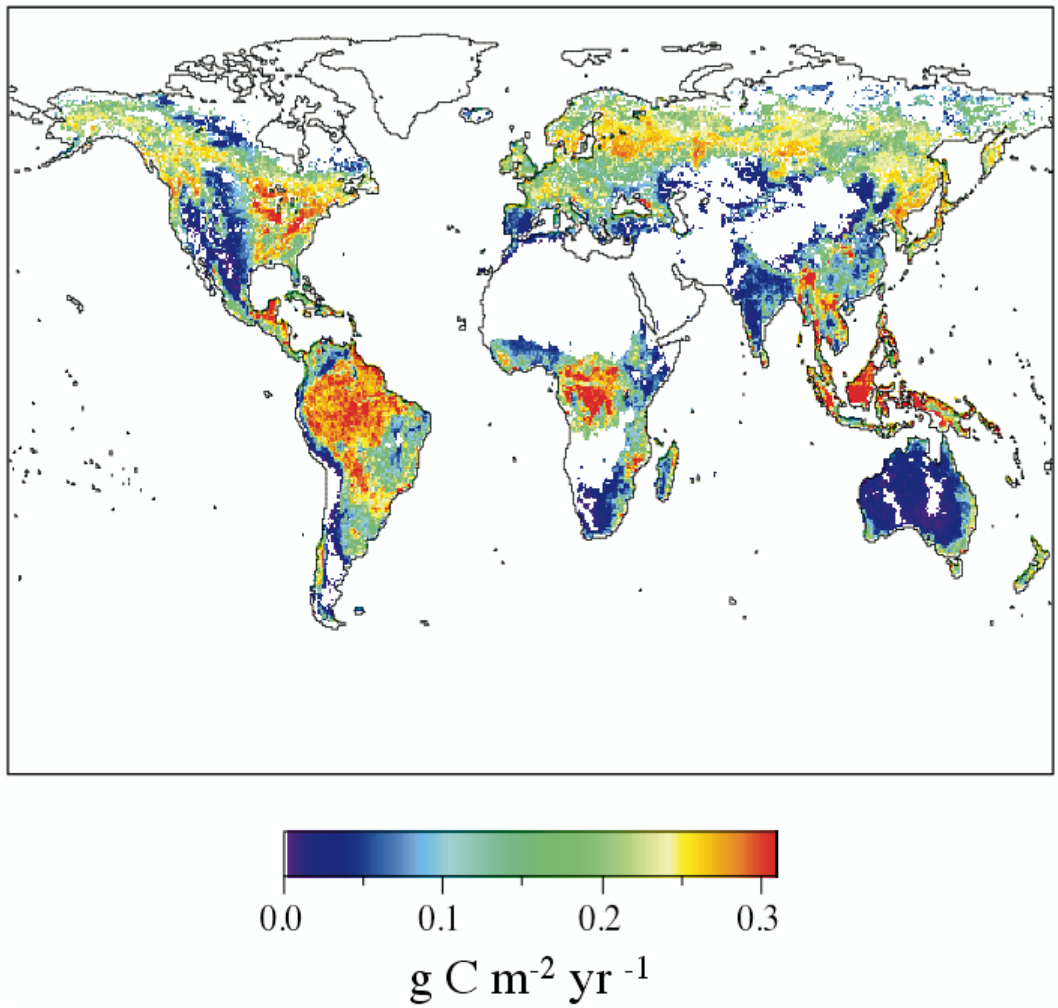

Figure 3. (*Continued*)

4. Discussion

The lower range value for our predicted emission total from live foliage (54 Tg yr^{-1}) accounts for the majority of previously postulated biogenic acetone sources in models of global atmospheric chemistry (Brasseur et al., 1998; Jacob et al., 2002). Singh et al. (Singh et al., 2000) estimated total global acetone emissions of 56 Tg yr^{-1}. In a global atmospheric study of acetone sources, Jacob et al. (Jacob et al., 2002) assumed a direct emission from live vegetation to be 20–40 Tg yr^{-1}, and an additional emission source of 9 Tg yr^{-1} from decaying plant residues worldwide. These estimates for dead foliage sources are close to our own predictions, but generally below the lower ends of our predicted flux ranges for acetone for both live and dead foliage sources. One possible explanation for this discrepancy is that Jacob et al. (Jacob et al., 2002) did not consider the high level

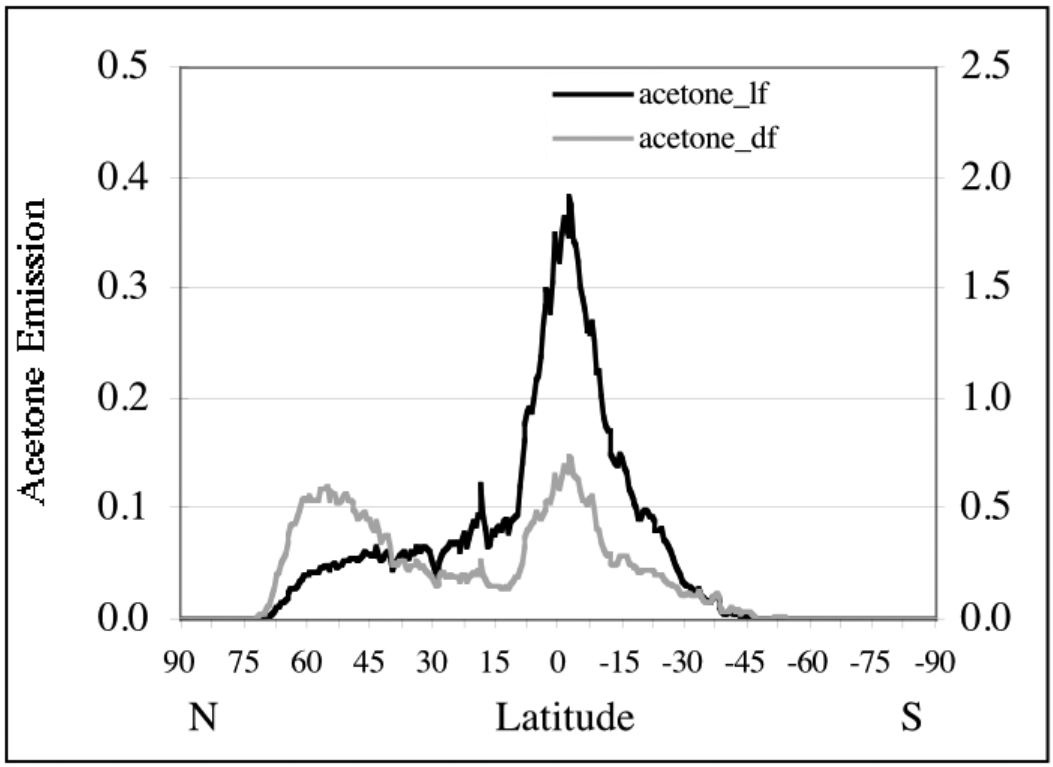

Figure 4. Predicted acetone emissions from live foliage (dark line, right axis) and dead foliage (light line, left axis) (in Tg C yr^{-1}) for 0.5 latitude zones.

of heteorogenity in foliar density observed by satellites across global ecosystems from tundra to grasslands to forests, nor from high latitudes to the moist tropical zones. Tropical evergreen forests have high LAI canopy levels of 4–6 year-round, which are exposed to fairly constant warm temperatures that may be conducive to elevated OVOC emission levels not routinely measured previously in (mostly temperate zone) ecosystems and plant species.

Another possible explanation for the high range in our predicted emission total of acetone from live foliage sources is the assumption of high and globally uniform ε values, derived from a small number of reported flux experiments in vegetation communities that are not representative of other plant species around the world. To expand the database of measured values, we are currently making new closed-chamber estimates of all parameters used in Equations (1)–(3) for acetone emissions from a variety of plant types, including broadleaf temperate and tropical tree species. In due time, representative measured values of ε and β for all land cover types listed in Table 2 will replace uniform settings for these terms in global model algorithms.

Other potential improvements in our global model for biogenic OVOC emissions will include confirmation and inclusion of measured effects of the following:

1. moisture stress and variable humidity levels on emissions from live foliage;
2. elevated acetone emissions from live foliage during the periods of bud break (i.e., triglyceride mobilization; Fall, 1999) or during leaf senescence; and
3. wetting and drying on emissions from decaying foliage.

It is worth noting that the actual escape efficiency of any VOC to the above-canopy air mass is not likely to be 100% (Guenther, 1999), which means that the leaf-to-canopy-level emission fluxes estimated in the model algorithms presented here account only for emission flux prior to (re)entrainment of OVOC by vegetation canopies. Subsequent field and airborne measurements are necessary to determine if the initial biogenic flux estimates we report from this modeling study are substantially diminished in magnitude prior to actual release into the free troposphere.

We conclude that predicted biogenic flux totals from our modeling approach are large enough to account for the majority of postulated acetone sources from land in global atmospheric budgets. Although more measurement data for biogenic OVOC fluxes will improve the vegetation-specific parameters in subsequent versions of the model, new global satellite observations of canopy leaf dynamics, which form the basis for our emissions approach, represent progress toward capturing important sources of variability in biogenic emissions over seasons and years.

Acknowledgments. This work was supported by the NASA Earth Observing System Interdisciplinary Science Program, Grant MDAR-0044–0126, to Christopher Potter, principal investigator.

References

Brasseur, G.P., D. A. Hauglustaine, S. Walters, P. J. Rasch, J.-F. Muller, C. Granier, and X. X. Tie, 1998: MOZART, a global chemical transport model for ozone and related chemical tracers. 1—Model description. *J. Geophys. Res.*, **103**, 28,265–28,289.

Buermann, W., J. Dong, X. Zeng, R. B. Myneni, and R. E. Dickinson, 2001: Evaluation of the utility of satellite-based vegetation leaf area index data for climate simulations. *J. Clim.*, **14**, 3536–3550.

Collins, W. J., D. S. Stevenson, C. E. Johnson, and R. G. Derwent, 1999: Role of convection in determining the budget of odd hydrogen in the upper troposphere. *J. Geophys. Res.*, **104**, 26,927–26,941.

DeFries, R., et al., 1995: Mapping the land surface for global atmosphere–biosphere models: Toward continuous distributions of vegetation's functional properties. *J. Geophys. Res.*, **100**, 20,867–20,882.

DeFries, R., M. Hansen, J. R. G. Townshend, and R. Sohlberg, 1998: Global land cover classifications at 8 km spatial resolution: the use of training data derived from Landsat imagery in decision tree classifiers. *Intl. J. Remote Sens.*, **19**, 3141–3168.

deGouw, J. A., C. Howard, T. Custer, and R. Fall, 1999: Emissions of volatile organic compounds from cut grass and clover are enhanced during the drying process. *Geophys. Res. Lett.*, **26**, 811–814.

Fall, R., 1999: Biogenic emissions of VOCs from higher plants. *Reactive Hydrocarbons in the Atmosphere*, edited by C.N. Hewitt, Academic Press, San Diego, 43–96.

Fall, R., T. Karl, A. Hansel, A. Jordan, and W. Lindinger, 1999: Volatile organic compounds after leaf wounding: On-line analysis by proton-transfer-reaction mass spectrometry. *J. Geophys. Res.,* **104**, 15,963–15,974.

Federer, C. A., 1979: A soil–plant–atmosphere model for transpiration and availability of soil water. *Water Resour. Res.,* **15**, 555–562.

Fukui, Y., and P. V. Doskey, 1998: Air-surface exchange of nonmethane organic compounds at a grassland site: Seasonal variations and stressed emissions. *J. Geophys. Res.,* **103**, 13,153–13,168.

Guenther, A., 1999: Modeling biogenic volatile organic compound emissions to the atmosphere. *Reactive Hydrocarbons in the Atmosphere,* edited by C. N. Hewitt, Academic Press, San Diego, 41–94.

Guenther, A., et al., 1995: A global model of volatile organic compound emissions. *J. Geophys. Res.,* **100**, 8873–8892.

Holben, B. N., 1986: Characteristics of maximum-value composite images from temporal AVHRR data. *Intl. J. Remote Sens.,* **7**, 1417–1434.

Holzinger, R., A. Jordan, A. Hansel, and W. Lindinger, 2001: Methanol measurements in the lower troposphere near Innsbruck (47°16'N; 11°24'E), Austria. *Atmos. Environ.,* **35**, 2525–2532.

Jacob, D. J., B. D. Field, E. M. Jin, I. Bey, Q. Li, J. A. Logan, R. M. Yantosca, and H. B. Singh, 2002: Atmospheric budget of acetone. *J. Geophys. Res.,* **107**(D10) 4100, doi:10.1029/2001JD000694.

Kirstine, W., I. Galbally, Y. Ye, and M. Hooper, 1998: Emissions of volatile organic compounds (primarily oxygenated species) from pasture. *J. Geophys. Res.,* **103**, 10,605–10,619.

Knyazikhin, Y., J. V. Martonchik, R. B. Myneni, D. J. Diner, and S. W. Running, 1998: Synergistic algorithm for estimating vegetation canopy leaf area index and fraction of absorbed photosynthetically active radiation from MODIS and MISR data. *J. Geophys. Res.,* **103**, 32,257–32,276.

Legates, D. R., and C. J. Willmott, 1990: Mean seasonal and spatial variability in global surface air temperature. *Theor. Appl. Climatol.,* **41**, 11–21.

Los, S. O., C. O. Justice, and C. J. Tucker, 1994: A global 1x1 NDVI data set for climate studies derived from the GIMMS continental NDVI data. *Intl. J. Remote Sens.,* **15**, 3493–3518.

MacDonald, R. C., and R. Fall, 1993: Acetone emissions from conifer buds. *Phytochemistry,* **34**, 991–994.

Malmström, C. M., M. V. Thompson, G. P. Juday, S. O. Los, J. T. Randerson, and C. B. Field, 1997: Interannual variation in global scale net primary production: Testing model estimates. *Global Biogeochem. Cycles,* **11**, 367–392.

Müller, J.-F., and G. Brasseur, 1999: Sources of upper tropospheric HO_x: A three-dimensional study. *J. Geophys. Res.,* **104**, 1705–1715.

Olivier, J. G. J., J. J. M. Berdowski, J. A. H. W. Peters, J. Bakker, A. J. H. Visschedijk, and J. P. J. Bloos, 2001: Applications of EDGAR. Including a description of EDGAR V3.0: Reference database with trend data for 1970–1995. RIVM, Bilthoven. *RIVM Rep. 773301 001/NRP Rep. 410200 051*, 159 pp.

Potter, C. S., J. T. Randerson, C. B. Field, P. A. Matson, P. M. Vitousek, H. A. Mooney, and S. A. Klooster, 1993: Terrestrial ecosystem production: A process model based on global satellite and surface data. *Global Biogeochem. Cycles*, **7**, 811–841.

Running, S. W., and R. R. Nemani, 1988: Relating seasonal patterns of the AVHRR vegetation index to simulated photosynthesis and transpiration of forests in different climates. *Remote Sens. Environ.,* **24**, 347–367.

Schade, G. W., and A. H. Goldstein, 2001: Fluxes of oxygenated volatile organic compounds from a ponderosa pine plantation. *J. Geophys. Res.,* **106**, 3111–3123.

Sellers, P. J., C. J. Tucker, G. J. Collatz, S. O. Los, C. O. Justice, D. A. Dazlich, and D. A. Randall, 1994: A global 1×1 NDVI data set for climate studies. Part 2: The generation of global fields of terrestrial biophysical parameters from the NDVI. *Intl. J. Remote Sens.*, **15**, 3519–3545.

Singh, H. B., M. Kanakidou, P. J. Crutzen, and D. J. Jacob, 1995: High concentrations and photochemical fate of oxygenated hydrocarbons in the global troposphere. *Nature*, **378**, 50–54.

Singh, H. B., et al., 2000: Distribution and fate of selected oxygenated organic species in the troposphere and lower stratosphere over the Atlantic. *J. Geophys. Res.*, **105**, 3795–3806.

Singh, H. B., Y. Chen, A Staudt, D. Jacob, D. Blake, B. Heikes, and J. Snow, 2001: Evidence from the Pacific troposphere for large global sources of oxygenated organic compounds. *Nature*, **410**, 1078–1081.

Warneke, C., T. Karl, H. Judmaier, A. Hansel, A. Jordan, W. Lindinger, and P. J. Crutzen, 1999: Acetone, methanol, and other partially oxidized volatile organic emissions from dead plant matter by a biological processes: Significance for atmospheric HO_x chemistry. *Global Biogeochem. Cycles*, **13**, 9–17.

Wennberg, P. O., et al., 1998: Hydrogen radicals, nitrogen radicals, and the production of ozone in the upper troposphere. *Science*, **279**, 49–53.